PAPER • OPEN ACCESS

Numerical Study for Open Reactor Design Using Salt Hydrate

To cite this article: A A Hawwash *et al* 2019 *IOP Conf. Ser.: Earth Environ. Sci.* **322** 012021

View the article online for updates and enhancements.

IOP ebooks™

Bringing you innovative digital publishing with leading voices to create your essential collection of books in STEM research.

Start exploring the collection - download the first chapter of every title for free.

This content was downloaded from IP address 156.213.245.110 on 24/09/2019 at 22:09

Numerical Study for Open Reactor Design Using Salt Hydrate

A.A. Hawwash[1,2,3]*, Shinsuke Mori[2], Khalid El Feky[1,] and Hamdy HASSAN[1,4]

1 Energy Resources Engineering Department, Egypt- Japan University of Science and Technology, Egypt.
2 Graduate school of science and engineering, Tokyo Institute of Technology, Japan.
3 Mechanical Engineering Department, Benha Faculty of Engineering, Benha University, Egypt.
4 Mechanical Engineering Department, Faculty of Engineering, Assiut University, Egypt.
E-mail: ahmed.hawash@ejust.edu.eg

Abstract. There are various methods to store thermal energy from season to season. Because the density of energy storage in thermochemical materials is higher than the latent and sensible heat storage method, the thermochemical heat storage is considered the sufficient type. This paper provides a mathematical model of thermochemical storage process for thermochemical materials; potassium aluminum sulfate 12-hydrate ($KAl(SO_4)_2.12H_2O$). The software used is COMSOL Multiphysics Modelling Software. The model data is validated and compared with the previous experimental result. Furthermore, the temperature difference and the pressure over the material inside the reactor are investigated. There are seven designs for the bed. However, the inlet and outlet diameter of the bed is changed; there is any change in the volume and height of the bed. The model results present that the rise in entrance area decreases the charging time and rises the pressure drop inside the material. Case 4 is the best design from the charge time.

1. Introduction

While the energy crises are getting worth, like, Global Warming phenomena and limited fossil fuel sources, Renewable energy, as an alternative solution, has been often used. However, the solar radiation is the most promising source in sustainable energy section; there is a challenge considered in the weakness of collected solar rays during the winter season. In Egypt, the energy required for the buildings demand is 51% of total power consumption [1], also the 50% of this consumption is consumed by the hot domestic water and space heating [2].

The long-term heat storage is considered a novel technique to store solar energy from summer to winter. It is a significant method to store a large amount of solar energy with high energy efficiency. Thus many authors pay their attentions for long time heat storage method [3–5]. The materials used are salt hydrates, and the reaction type is thermochemical reaction [6]. Since the salt hydrates exposed to waste energy or solar radiation during the summer period, it will be charged with thermal energy and produce vapor. Then, the anhydrite salt is stored for a long time until cooling weather, and the sensible heat can be released from salt during the hydration process. There are three main types of thermal energy storage; Latent Heat Storage (LHS), Thermochemical Heat Storage (THS) and Sensible Heat Storage (SHS). Compared with LHS and SHS, the energy density of Thermochemical Heat Storage is the highest, about 200–500 kWh m^{-3} [7]. During the storage period, the heat losses of THS is ignored because of the absorbed energy is stored in chemical potential [4].

Content from this work may be used under the terms of the Creative Commons Attribution 3.0 licence. Any further distribution of this work must maintain attribution to the author(s) and the title of the work, journal citation and DOI.
Published under licence by IOP Publishing Ltd

Nomenclature

Symbol	Description	Symbol	Description
C [J/(kg.K)]	specific heat	**T [K]**	Temperature
C_f	Dimensionless form-drag constant	**u [m/s]**	Fluid velocity
C_p [J/(kg.K)]	specific heat at constant pressure	**v [m/s]**	Inlet air velocity for the reactor
E_a [J/mol]	Activation energy	**ρ [kg/m^3]**	Density
h [m]	Reactor height	**μ [Pa.s]**	Dynamic viscosity
ΔH [J/kg]	Heat of the reaction	ξ_w	water vapor mass fraction
K [m2]	specific permeability	**Ɛ**	void fraction of the bed
K [W/ (m.K)]	Thermal conductivity	**τ [s]**	Overall reaction time
∇P **[Pa]**	pressure drop	**ε**	Material porosity
t [s]	Time		

Commonly, the thermochemical reaction without sorption and with chemisorption are the main two types of Thermochemical Heat Storage [8], and the first type is a reversible exo/endo-thermic reaction took place between two thermochemical substances, where a significant amount of thermal heat energy is stored or generated. Furthermore, the reaction progression of hydration and dehydration process is complicated besides by-product could be formed [9–15]. Consequently, screening salt hydrate method rely on factors [16]; salt corrosiveness, (2) operating pressure inside reactor, (3) salt sustainability, (4) salt recyclability, (5) environmental safety and the toxicity of the thermochemical material, (6) material cost, (7) salt energy density, (8) charging and hydration temperature range and (9) salt stability during hydration and dehydration.

The sorption thermal energy storage systems are considered promising for solar energy field [17], due to their advantage of high energy density and the function to preserve energy for long time with limited energy loss. The disadvantages of thermochemical salt material are [18]; (1) low recyclability, (2) low rate of heat and mass transfer, and (3) the formation of layer-like gel formed during hydration at the inlet of the bed. The reversible reaction happened during hydration and charging for salt materials in specific conditions, is exo/endothermic reaction. In another mean, thermochemical materials release and store thermal energy via hydration and charging chemical reaction [20].

Donkers et al. [19] screened 262 salts (536 thermochemical reactions), and then defined the limitations of all salt hydrate used in the environment. The evaluation depends on three criteria; (1) during hydration reaction, 50 ℃ was the minimum temperature of the outlet fluid, (2) the maximum dehydration temperature was 120 ℃ and (3) the hydration reaction capacity was 1.3 GJ/m^3 at least. Consequently, the salt materials shortlist contains 25 thermochemical materials based on this filter. They concluded that K_2CO_3 is the most promising thermochemical materials.

A. Rubino and R. Boer [20] built a simulation model for an open thermochemical storage system. COMSOL Multiphysics Software was used to analyze the model in both time and space by solving algebraic and partial deferential equations. The model result was validated with experimental results which magnesium chloride hexahydrate is the salt material for dehydration and hydration process. The model used to define the best reactor design related to heat storage efficiency during charging.

Marias et al. [21] achieved an open thermochemical storage setup and examined two porous thermochemical materials; Aluminium potassium sulfate hydrate ($KAl(SO_4)_2.3\text{-}12H_2O$) and $SrBr_2.6H_2O$. Beside they studied experimentally the dehydration and hydration process, they developed a theoretical model to expand the result and predict outlet air temperature when the inlet conditions are identified. They show the hydration and dehydration operating line. They illustrated that the effectiveness of thermochemical reaction depends on the salt material type and equals 0.8/0.9 and 0.5/0.6 for $SrBr.6H_2O$ and $KAl(SO_4)_2.12H_2O$.

In a recent study, potassium aluminum sulfate hydrate is used and selected due to the required charging temperature is appropriate for a solar application like flat plate solar collectors and evacuated tube collectors, and the outlet temperature during hydration is suitable with domestic applications [22-24]. However, the literature shows different research areas focused on long-term heat storage; the published papers developed the reactor design is not found. In addition, there is no work study the improving dehydration and sorption time. Recent study aims to examine theoretically the effect of reactor design on the thermal performance of open thermochemical storage system, using potassium aluminum sulfate 12-hydrate. Since the volume and the height of the reactor are constant, the design varies in inlet and outlet diameter of the reactor. Hence, charging and hydration time will be studied. Furthermore, the temperature at the outlet and inlet and pressure drop inside bed will be discussed. A 3D model for an open thermochemical storage system is developed using COMSOL Multiphysics Modelling Software to investigate the sorption and dehydration processes. Thus, based on the comparison between all design, we can define the optimum reactor.

2. Numerical analysis

The recent study investigates and simulates an open system of thermochemical heat storage due to the closed, evacuated system is complicated and required higher cost in case of experimental compared with the open atmospheric system [7]. During desorption or dehydration, the hot gases stream passes through the totally hydrated porous materials inside the reactor, leading to an endothermic reaction. In this model, the Reynolds number is lower than 10, and the stream flow inside the bed is laminar, thus Brinkman equation is applied. All parameters and material properties used in the simulation is indicated in Table.1.

Table 1. The properties and parameters used in the numerical simulation [22, 30].

Symbol	Value	Unit	Description
K	0.7e-9	m^2	Material permeability
ε	0.7		Material porosity
K_{ins}	0.05	W/ (m.K)	Insulation thermal conductivity
K_m	0.704	W/(m.K)	Salt thermal thermal conductivity
ρ_b	1757	kg/m^3	Bulk density
T_{in}	25-65	℃	Inlet air temperature for the reactor
T_{amb}	25	℃	Ambient air temperature
v	0.1	m/s	Inlet air velocity for the reactor
D_w	2.6e-5	m^2/s	Water- air diffusivity
E_a	55	[kJ/mol]	Activation energy
C_p	456	J/(kg.K)	Heat capacity at constant pressure
E_d	409	$kW.h/m^3$	Energy density

2.1. Geometry and Model Implementation

In our study, 7 reactor designs are investigated numerically for ($KAl(SO_4)_2.12H_2O$) dehydration process. The parameters which have change are entrance and outlet area of the reactor, but the reactor height and volume are constant at 22 cm and $20x10^{-3}$ m^3 respectively. Figure. 1. displays the schematic diagram of cylindrical reactor (1st case) and operating conditions which used in the model. Table.2 indicates the dimension of seven designs.

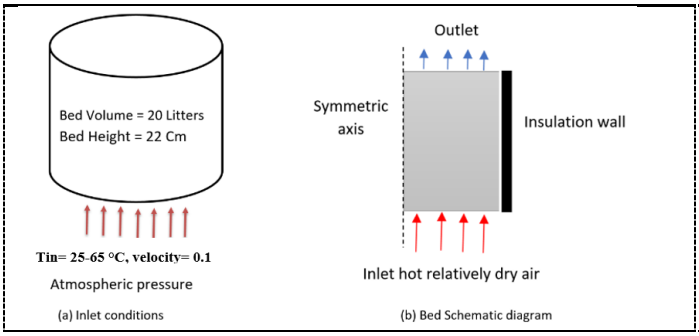

Figure 1. The model inlet conditions and the Bed schematic diagram

Table 2. The dimension data for studied cases of the reactor.

Symbol	Case 1	Case 2	Case 3	Case 4	Case 5	Case 6	Case 7
a: the inlet (cm)	17	18.4	20.949	22	15.5	10.47	9.125
b: the outlet (cm)	17	15.5	10.47	9.125	18.4	20.949	22
	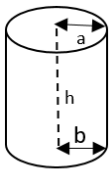	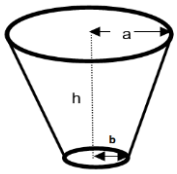			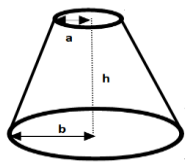		

2.2. Equations and mathematics

The general equation for the reversible reaction between a gas and a salt is [3] and [22–31];

$$C + Heat \leftrightarrow A + B \tag{1}$$

and the reversible thermochemical reactions for $KAl(SO_4)_2.\ 12H_2O$ is;

$$KAl(SO_4)_2.12H_2O_{(s)} + 44{,}192 J/mol_w \Leftrightarrow KAl(SO_4)_2.3H_2O_{(s)} + 9H_2O_{(g)} \tag{2}$$

and the mass conservation between vapor and salt material is [20];

$$\varepsilon\rho_f \frac{\partial \xi}{\partial t} + \rho_F (u.\nabla)\xi_w = r_w \tag{3}$$

$$(1-\varepsilon)\frac{\partial \rho_s}{\partial t} = -r_w \tag{4}$$

Where, m_w, r_w, m_{da}, ξ_w and ε are vapor mass, water absorption reaction rate, dry air mass, vapor mass fraction, and bed void fraction respectively. Brinkman equations is;

$$\rho\frac{\partial u}{\partial t} = \nabla\left[-PI + \mu\frac{1}{\varepsilon_p}(\nabla u) - \frac{2}{3}\mu\frac{1}{\varepsilon_p}(\nabla u)I\right] - \left(\mu k^{-1} + B_f|u| + \frac{Q_{br}}{\varepsilon_p^2}\right)u \tag{5}$$

and the energy balance between the salt solid and fluid is;

$$(1-\varepsilon)\rho_s C_s \frac{\partial T_s}{\partial t} = (1-\varepsilon)k_s\nabla^2 T_s + q_s''' \tag{6}$$

$$\varepsilon\rho_F C_{pF}\frac{\partial T_F}{\partial t} + \rho_F C_{pF} u.\nabla T_F = \varepsilon k_s \nabla^2 T_s \tag{7}$$

It is assumed that $T_s = T_f = T$, so the thermal equilibrium between gas and solid is;

$$(\rho C)_m \frac{\partial T}{\partial t} + (\rho C)_F (u.\nabla)T = k_m \nabla^2 T + q_s''' \tag{8}$$

Where q''' and C_p are the rate of heat source related to volume unit and specific heat at constant pressure respectively. The reactor heat source rate is;

$$q_s''' = \Delta H.r_w \tag{9}$$

where Δ H and r_w are the heat of reaction and the rate of reaction. The reaction rate for dehydration is [32];

$$r_w = -C_a \exp(-\frac{E_a}{RT_s})(\frac{P_F - P_{eq}}{P_{eq}}) \tag{10}$$

Where E_a and P_f, are activation energy and fluid pressure severally, and C_a and P_{eq} are the pre-exponential constant and equivalent pressure respectively. Figure 2 illustrates the equilibrium curve, which explains the relationship between vapor pressure, temperature for potassium aluminum sulfate hydrate [21].

3. Numerical Solution

COMSOL Multiphysics Modelling Software 5.3a is used to build the numerical model of the current open thermochemical system. The main components inserted in the software are; Heat Transfer in Porous Media, Brinkman equations, Transport of Diluted Species in Porous Media, Multiphysics and Chemistry. There are two types of coupling inside Multiphysics component; (1) temperature coupling and (2) flow coupling. Additionally, a test for mesh independent is illustrated. The recent result is validated with the experimental results [21] to certify the model result. Figure. 3 shows the validation of recent simulation with dehydration test [33], using Aluminium potassium sulfate 12-hydrate. The condition of the experimental and the physical and chemical properties of Aluminium potassium sulfate 12-hydrate are considered in the model. It is noticed that a reasonable agreement between the experimental result and the model result, also the error at the end of the dehydration test is not increased than 8 %.

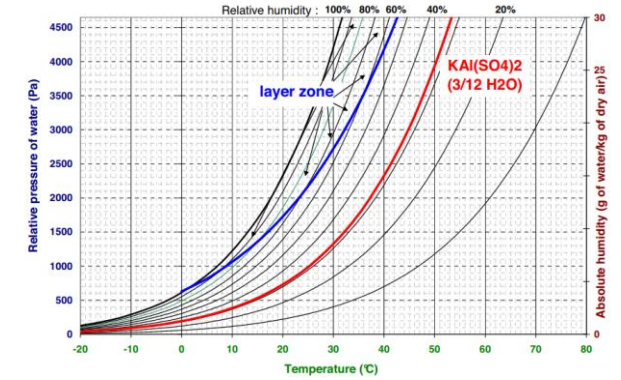

Figure 2. potassium aluminum sulfate 12-hydrate equilibrium curve in a psychometric chart.

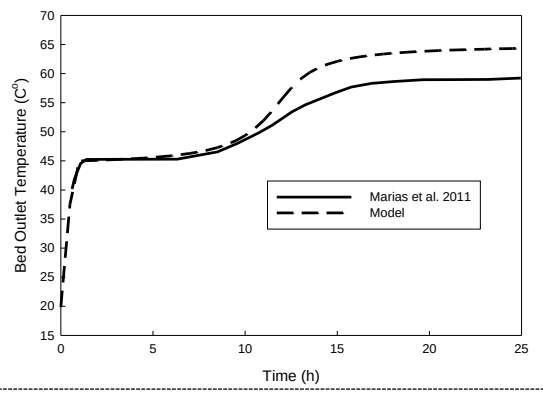

Figure 3. The validation curve related to bed outlet temperature in the model.

4. Result and Discussions

In the current study, two reactor configurations are studied; cylindrical design and truncated cone. The inlet and outlet diameter of the bed is changed parallel with no change in the total volume and height. The dehydration process for ($KAl(SO_4)_2.12H_2O$) start when hot air enters the reactor at room temperature and increases dramatically with the rate of 1 (℃/min), until reaches the peak temperature 65 ℃, and be constant at this point. The dehydration process of ($KAl(SO_4)_2.12H_2O$) happens in one step, as shown in the charging line in Figure 4. We can note that the dehydration operating time in case.4 is the lowest at 11.5 hours, compared with cases 3, 2, and 1 around 13, 20, and 25 hours respectively. The increasing entrance diameter decreases the operating time of dehydration. Furthermore, the figure displays that cases 3 and 4 are better than case 1 and 2 related to the dehydration time. The dehydration time is an important factor for the open thermochemical storage system when the solar air collector is the source of hot air. In addition, after 33 hours of charging potassium aluminum sulfate hydrate, both case 3 and 4 reach about 90% dehydrated, compared with case 1. Hence, the cylindrical design is not suitable to design due to the longer charging time.

The pressure drop is important to factor in thermochemical heat storage systems during dehydration. Figure 5 illustrates the variation of pressure through potassium aluminum sulfate hydrate with time, during charging for cases 1,2,3 and 4. It is noted that the pressure drop rises with operating time, due

to the declining in vapor content inside the ($KAl(SO_4)_2.12H_2O$) reaching to ($KAl(SO_4)_2.3H_2O$) which reduces the material porosity. Nevertheless, the charging time is decreased when the design change from case1 to case 4, but the pressure drop inside the reactor increased. The increasing in pressure drop means higher operating cost. Hence, case 4 is chosen as the dehydration time is a significant factor in the thermochemical heat storage system, especially when the solar collector is the source of heat [33-35]. Overall, the pressure drop rises with increasing in the bed entrance diameter.

Figure 6 illustrates the temperature difference between the outlet and inlet gas with time for cases 1, 5, 6, and 7. The figure reveals the percentage of charging process with time, since first design reaches full dehydrate early via the shortest operating time, compared with cases 5, 6, and 7. The gas inlet temperature rises from 25 ℃ until 65 ℃ with a rate of 1 K/s. It is revealed that Cases 1, 5, 6 and 7 require more time to reach full hydrated or they need more cost.
Figure 7 displays the pressure drop for cases 1, 5, 6, and 7 with operating time for the dehydration process. It is seen that the rate of the pressure drop grow is various for cases 1, 5, 6, and 7. Additionally, case 7 has the lowest pressure drop, which means that a lower blower power required to flow the air inside the bed. While, the pressure drop average in case 6 is approximately half of case 1, the rising rate in pressure drop of case 6 and 7 is one third lower than case 1. Although, the pressure drop difference between cases 6 and 5 is the largest one. Furthermore, the dehydration reaction time in case 1 and 5 is approximately the same, because the pressure difference between the two cases is not big enough to affect significantly on the dehydration time.

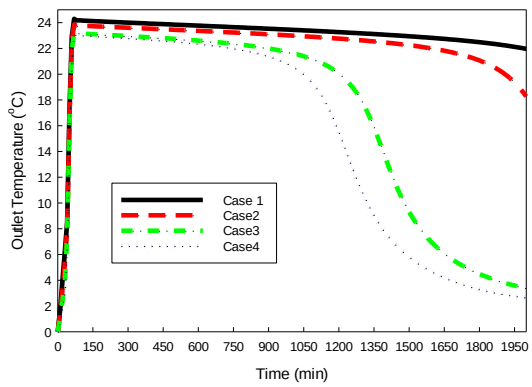

Figure 4. The temperature difference between inlet and outlet gas stream for cases 1, 2, 3, and 4 of reactor design for potassium aluminum sulfate hydrate.

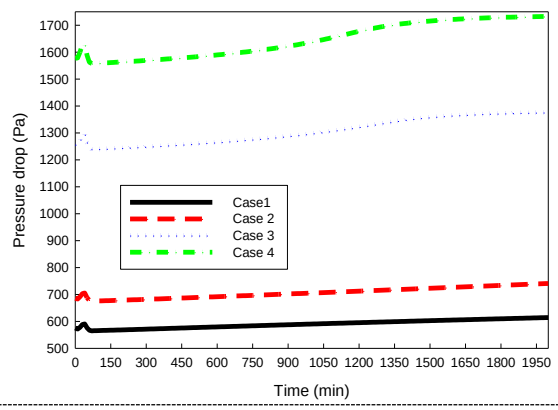

Figure 5. The pressure drop for cases 1, 2, 3, and 4 for the reactor design contains potassium aluminum sulfate hydrate.

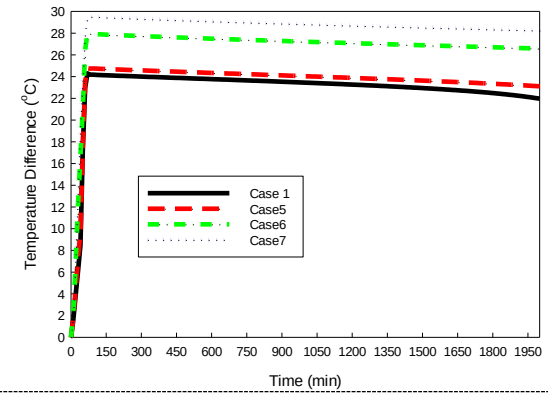

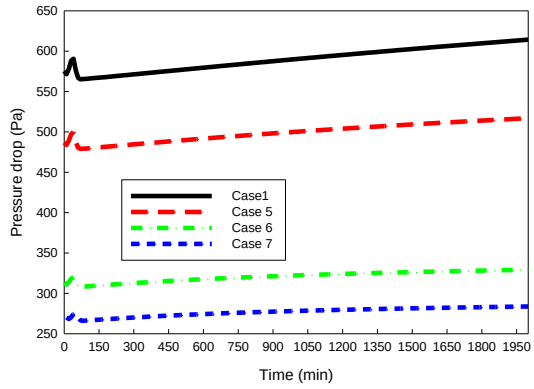

Figure 6. The temperature difference between inlet and outlet gas stream for cases 1, 5, 6, and 7 of reactor design contains potassium aluminum sulfate hydrate.

Figure 7. The pressure drop for case1, 5, 6, and 7 for the reactor design contains potassium aluminum sulfate hydrate.

Figure 8 shows the pressure drop distribution through potassium aluminum sulfate hydrate for cases 1, 4, and 7. It is significantly seen that the pressure at the outlet is lower than the entrance since there is a flow resistance faces the gas flow and increases along with the porous media. It is revealed that there is a significant difference in the pressure drop inside the reactor of all cases during the dehydration process. The pressure difference between inlet and outlet of the reactor at 300 Pa, 600 Pa, and 1830 Pa for case 7, case 1 and case 4, respectively. It means that from the pressure drop point of view, case 4 is the worst case compared with Cases 1 and 7.

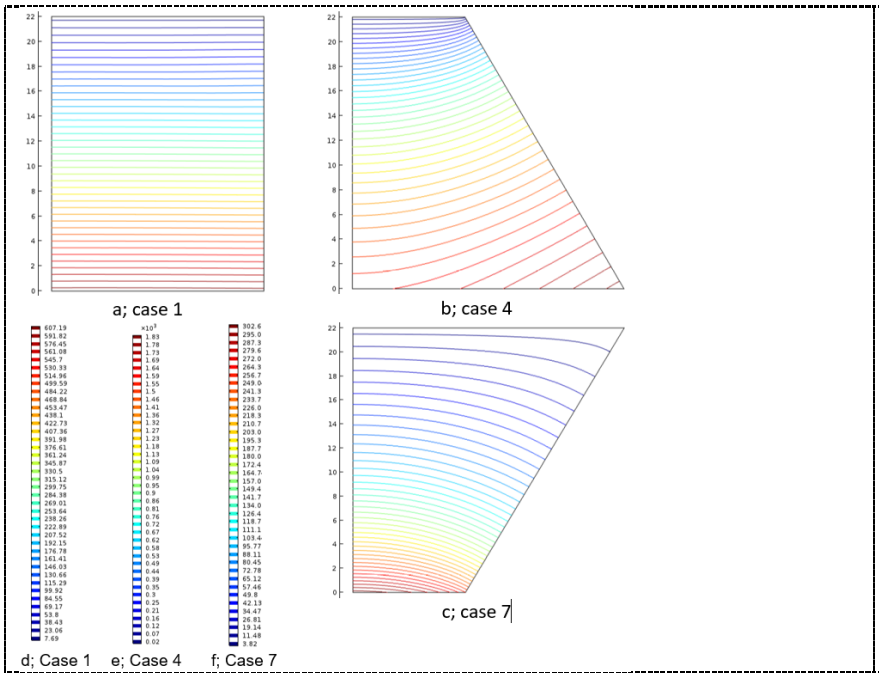

Figure 8. The pressure distribution inside the reactor contain potassium aluminum sulfate hydrate after 2000 min of dehydration for; a: case 1, b: case4 and c: case7, also the pressure scale for d; case 1, e; case 4 and f; case 7.

5. Conclusion

During the dehydration process for potassium aluminum sulfate hydrate, the influence of variation in the entrance and outlet area of the bed on charging time and the pressure drop inside salt hydrate is investigated. In addition, the volume and height of the reactor are fixed. On the one hand, a comparison between seven designs displays that the rise in entrance diameter increases the pressure drop and decreases the charging time. On the other hand, the entrance diameter decreasing reduces the pressure drop and decelerates the charging time. Case 4 is the best design as time is the main factor in the open thermochemical system. Case 7 can be used when the heat source is operating at a lower heating rate.

6. References

[1] S. H. Osman, Mediterr. Energy Regul., (2015).
[2] R. Parameshwaran, S. Kalaiselvam, S. Harikrishnan, and A. Elayaperumal, Renew. Sustain., Energy Rev., 16, 2394–2433, (2012).
[3] L. K. Edem Liu, N'Tsoukpoe, Hui Le Pierrs, Nolwenn Luo, Renew. Sustain. Energy Rev., 13, 2385–2396, (2009).
[4] P. Pinel, C. A. Cruickshank, I. Beausoleil-Morrison, and A. Wills, Renew. Sustain. Energy Rev., 15, 3341–3359, (2011).
[5] P. Tatsidjodoung, N. Le Pierrès, and L. Luo, Renew. Sustain. Energy Rev., 18, 327–349, (2013).

[6] G. Balasubramanian, M. Ghommem, M. R. Hajj, W. P. Wong, J. A. Tomlin, and I. K. Puri, Int. J., Heat Mass Transf., 53, 5700–5706, (2010).
[7] B. Michel, P. Neveu, and N. Mazet, Energy, 72, 702–716, (2014).
[8] B. Wu, H. Ma, Z. Pan, J. Wang, W. Qu, and B. Wang, Int. Agric. Eng. J., 23, 70–79, (2014).
[9] A. E. Kalyva et al., Int. J. Hydrogen Energy, 42, 9533–9544, (2017).
[10] J. Lu, Y. Chen, J. Ding, and W. Wang, Appl. Energy, 162, 1473–1482, (2016).
[11] S. Tescari et al., Energy Procedia," 49, 1034–1043, (2013).
[12] Y. Kato, T. O-shima, and Y. Yoshizawa, Int. J. Energy Res., 25, 577–589, (2001).
[13] M. Jin, P. Frohberg, Y. Sun, P. Li, J. Yu, and J. Ulrich, Chem. Eng. Sci., 133, 181–189, (2014).
[14] Y. Yoshizawa, Appl. Therm. Eng., 16, 853–862, (1996).
[15] F. Schaube, L. Koch, A. Wörner, and H. Müller-Steinhagen, Thermochim. Acta, 538, 9–20, (2012).
[16] K. E. NTsoukpoe, T. Schmidt, H. U. Rammelberg, B. A. Watts, and W. K. L. Ruck, Appl. Energy, 124, 1–16, (2014).
[17] P. Pardo, A. Deydier, Z. Anxionnaz-Minvielle, S. Rougé, M. Cabassud, and P. Cognet, Renew. Sustain. Energy Rev., 32, 591–610, (2014).
[18] D. Aydin, S. P. Casey, and S. Riffat, Renew. Sustain. Energy Rev., 41, pp. 356–367, (2015).
[19] P. A. J. Donkers, L. C. Sögütoglu, H. P. Huinink, H. R. Fischer, and O. C. G. Adan, Appl. Energy, 199, 45–68, (2017).
[20] A. Rubino and R. de Boer, 10th IIR Gustav Lorentzen Conf. Nat. Refrig., 1–8, (2012).
[21] F. Marias, P. Neveu, G. Tanguy, and P. Papillon, CEA, 66, 4907–4918, (2017).
[22] A. Fopah Lele, F. Kuznik, O. Opel, and W. K. L. Ruck, Energy Convers. Manag., 106, 1327–1344, (2015).
[23] M. Richter, E. M. Habermann, E. Siebecke, and M. Linder, Thermochim. Acta, 659, 136–150, (2018).
[24] A. Fopah-Lele, F. Kuznik, T. Osterland, and W. K. L. Ruck, Appl. Therm. Eng., 101, 669–677, (2016).
[25] B. Michel, N. Mazet, and P. Neveu, Appl. Energy, 129, 177–186, (2014).
[26] G. Tanguy, F. Marias, S. Rouge, J. Wyttenbach, and P. Papillon, Energy Procedia, 30, 388–394, (2012).
[27] F. Marias, Eurotherm Semin., 93, 1–20, (2011).
[28] H. U. Rammelberg, T. Schmidt, and W. Ruck, Energy Procedia, 30, 362–369, (2012).
[29] W. Chen, W. Li, and Y. Zhang, Appl. Therm. Eng., 135, 95–108, (2018).
[30] H. Zondag et al., Energy, (2008).
[31] V. Mamani, A. Gutiérrez, and S. Ushak, Sol. Energy Mater. Sol. Cells, 176, 346–356, (2018).
[32] M. Lebrun and B. Spinner, Chem. Eng. Sci., 45, 1743–1753, (1990).
[33] A. A. Hawwash, Ali K. Abdel-Rahman, S. Ookawara and S. A. Nada. JET, 4, 123–131, (2016).
[34] A. A. Hawwash, Ali K. Abdel-Rahman, S. Ookawara and S. A. Nada. Appl. Therm. Eng., 130, 363–374, (2018).
[35] A. A. Hawwash, Ali K. Abdel-Rahman, S. Ookawara and S. A. Nada. Energy procedia, 141, 310–314, (2017).

Acknowledgments
It is a pleasure to acknowledge that Tokyo Institute of Technology, Tokyo, Japan and and Egypt-Japan University of Science and Technology provide and support this study. Also, it is a pleasure to acknowledge Ministry of Higher Education (MoHE) of Egypt for providing a scholarship. They offering the facilities, tools and equipment needed to conduct this research work.